Study of the effect of the chromophore and nuclearity on the aggregation and potential biological activity of gold(I) alkynyl complexes.

Raquel Gavara,[a] Elisabet Aguiló,[a] Julia Schur,[b] Jordi Llorca,[c] Ingo Ott[b] and Laura Rodríguez[a,*]

[a] *Departament de Química Inorgànica, Universitat de Barcelona, Martí i Franquès 1-11, 08028 Barcelona, Spain. Tel. +34 934039130. E-mail: laura.rodriguez@qi.ub.es*

[b] *Institute of Medicinal and Pharmaceutical Chemistry, Technische Universität Braunschweig, Beethovenstrasse 55, 38106 Braunschweig, Germany*

[c] *Institut de Tècniques Energètiques i Centre de Recerca en NanoEnginyeria, Universitat Politècnica de Catalunya, Diagonal 647,08028 Barcelona, Spain.*

Abstract

The synthesis and characterization of four organometallic gold(I) complexes containing different water soluble phosphanes (TPPTS, PTA and DAPTA) and chromophoric units (4-pyridylethynyl and propargyloxycoumarin) is here reported. The analysis of their absorption and emission spectra led us to attribute their luminescent behaviour to the chromophoric organic ligands. Moreover, the presence of the gold(I) metal atom has been observed to be the responsible of an efficient intersystem crossing process responsible for the observed phosphorescence emission. Broad emission bands are observed in most cases due to the formation of organized aggregates in solution in agreement with microscopic characterization.

Biological activity of the complexes showed very low effects against tumor cell growth but an inhibitory potency against thioredoxin reductase (TrxR). The missing / low cytotoxic effects could be related to a low bioavailability as determined by atomic absorption spectroscopy.

Keywords: gold, alkynyl, thioredoxin reductase, cytotoxicity, luminescence

1. Introduction

Gold based compounds form a new family of cytotoxic agents of great interest as metallodrugs and the lead compound auranofin is currently undergoing clinical trials in the US as an anticancer agent. Nevertheless, the precise mechanisms of antitumor activity of gold compounds have not been completely understood yet.[1,2] The mechanistic studies show that in general DNA is not the main target[3] and the selenoenzyme thioredoxin reductase, a putative and now partially validated main target for many cytotoxic gold compounds,[4-10] although other mechanisms besides TrxR inhibition might contribute to the biological profile (*e.g.*, interactions with G-quadruplexes).[11-14] In particular, gold-phosphine compounds were investigated after the antiarthritic drug auranofin (thiolate–Au-PEt_3complex) and were found to present biological activity against different cancer cells. A series of auranofin analogues containing thiolate ligands were prepared, as well as bis(phosphine)Au(I), phosphane–gold-halides and phosphine-gold-alkynyl complexes.[15] Solubility is always an issue for drug administration, which is a limit that many potential anticancer metal complexes have to overcome. Flanking the phosphine with an appropriate co-ligand yields active complexes and both the steric and electronic properties appear to be important in the design of effective gold complexes.[16] The resulting solubility could be also tuned. It was also observed that the presence of a direct metal-carbon bond in Au(I) and Au(III) complexes appears to be rather beneficial for their stability and speciation in aqueous solutions. For this, various organometallic gold complexes were synthesized in which the presence of a direct carbon-gold bond greatly stabilizes the gold oxidation state and guarantees more controlled chemical speciation in biological systems.[17] Among organometallic gold(I) complexes, recent initial reports on the bioactivity of alkynyl gold complexes indicate that this type of complexes offers opportunities for the

development of new chemotherapeutics against cancer and infectious diseases. Despite their potential, only very few studies on the biological potential of alkynyl gold complexes have been reported so far.[18-23] Moreover, gold alkynyl complexes are well-known to display interesting luminescent properties that have been an interesting tool within the biological point of view among others.[24] Of note, gold(I) alkynyl derivatives containing the water-soluble 1,3,5-triaza-7-phosphaadamantane (PTA) and 3,7-diacetyl-1,3,7-triaza-5-phosphabicyclo[3.3.1]-nonane (DAPTA) phosphane ligands are cytotoxic in cancer cells and their cellular uptake was confirmed by fluorescence microscopy using the luminescent properties of these organometallics.[18] These phosphanes are particularly appealing due to their solubility in water that increases the global solubility of the complexes in this medium.

Recently, we reported on the luminescence and biological properties of a series of Au(I) alkynyl complexes containing the water soluble phosphanes PTA and DAPTA and a strong inhibition of the TrxR enzyme was observed.[23] Their observed gel formation in water could be also considered to investigate as a possible effect to affect the drug transfer through the cell membrane.[25-27] Following the previous studies, we have designed new water soluble complexes with some differences on their chemical structure (Chart 1) in order to analyze how these chemical modifications could affect both on their luminescent and biological properties.

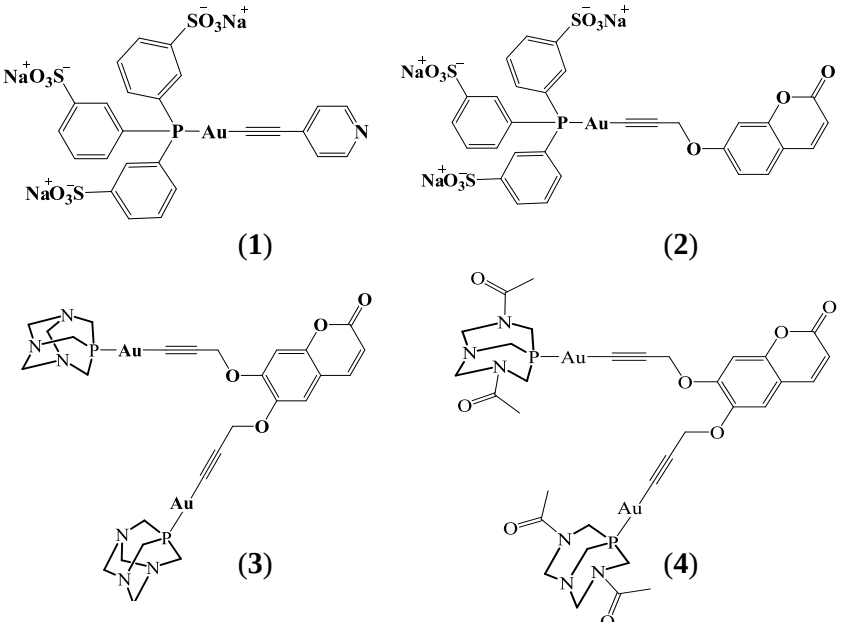

Chart 1

2. Experimental Section

2.1. General procedures

All manipulations were performed under prepurified N_2 using standard Schlenk techniques. All solvents were distilled from appropriated drying agents. Commercial reagent triphenylphosphine-3,3',3"-trisulfonic acid trisodium salt (TPPTS, Aldrich, 95%), 1,3,5-triaza-7-phosphaadamantane (PTA, Aldrich 97%) and 3,7-diacetyl-1,3,7-triaza-5-phosphabicyclo[3.3.1]nonane (DAPTA, Aldrich 97%) were used as received. Literature methods were used to prepare 4-ethynylpyridine,[28] Na_3[AuCl(TPPTS)],[29] [AuCl(PTA)],[30] [AuCl(DAPTA)],[30] 7-(prop-2-in-1-yloxy)-1-benzopyran-2-one[23] and $[Au(C{\equiv}Cpy)]_n$.[31] PBS: phosphate buffered saline pH 7.4; cell culture medium: minimum essential medium eagle; 30 % Danieau medium: 58 mM NaCl, 0.7 mM KCl, 0.4 mM $MgSO_4$, 0.6 mM $Ca(NO_3)_2$ and 5 mM HEPES (pH 7.2).

2.2. Physical measurements

Infrared spectra were recorded on a FT-IR 520 Nicolet Spectrophotometer. ^{1}H-NMR (δ(TMS) = 0.0 ppm), $^{31}P\{^1H\}$-NMR (δ(85% H_3PO_4) = 0.0 ppm) spectra were obtained on a Varian Mercury 400, Bruker 400 and Bruker DMX 500. ESI spectra were recorded on a Fisons VG Quatro spectrometer. Absorption spectra were carried out on a Varian Cary 100 Bio UV- spectrophotometer and emission spectra on a Horiba-Jobin-Ybon SPEX Nanolog spectrofluorimeter. Emission quantum yields were measured at 298 K relative to quinine sulphate (ϕ_F = 0.54, H_2SO_4 1N) for compound **1** and 7-methoxy-4-methylcoumarin as a reference (ϕ_F = 0.124, methanol) for compounds **2**-**4**, in water. Optical microscopy was recorded on an Olympus BX51. Scanning electron microscopy was carried out a 5kV using a Neon40 Crossbeam Station (Zeiss) equipped with a field

emission gun. A MALVERN Zetasizer Nano S operating at 173° scattering angle and 25 °C was used to perform the dynamic light scattering (DLS) measurements.

2.3. HR-CS AAS measurements

A contrAA© 700 high-resolution continuum source atomic absorption spectrometer (Analytik Jena AG) was used for the gold quantification in cell lysates. Gold was measured at a wavelength of 242.7950 nm. Samples were injected at a volume of 20 µl into coated standard graphite tubes AnalytikJena AG). Calibration was done in a matrix matched manner and pure samples of the gold complexes were used to prepare the standard solutions. The mean integrated absorbances (AUC = area under the curve) of triple injections were used throughout the study.

2.4. TrxR inhibitory effects

To determine the inhibition of TrxR an established microplate reader based assay was performed with minor modifications.[32] For this purpose commercially available thioredoxin reductase from rat liver (Sigma-Aldrich) was used and diluted with distilled water. The compounds were freshly dissolved as stock solutions in DMF. To each 25 µl aliquots of the enzyme solution each 25 µl of potassium phosphate buffer pH 7.0 containing the compounds in graded concentrations or vehicle (DMF) without compounds (control probe) were added and the resulting solutions (final concentration of DMF: max. 0.5% V/V) were incubated with moderate shaking for 75 minutes at 37°C in a 96 well plate. To each well 225 µl of reaction mixture (1000 µl reaction mixture consisted of 500 µl potassium phosphate buffer pH 7.0, 80 µl 100 mM EDTA solution pH 7.5, 20 µl BSA solution 0.2%, 100 µl of 20 mM NADPH solution and 300 µl of distilled water) were added and the reaction was started by addition of 25 µl of an 20 mM ethanolic dithio-bis-2-nitrobenzoic acid (DTNB) solution. After proper mixing,

the formation of 5-thio-2-nitrobenzoic acid (5-TNB) was monitored with a microplate reader (Perkin Elmer Victor X4) at 405 nm in 35 s intervals for 350 s. For each tested compound the non interference with the assay components was confirmed by a negative control experiment using an enzyme free solution. The IC_{50} values were calculated as the concentration of compound decreasing the enzymatic activity of the untreated control by 50% and are given as the means and error of 2 - 3 independent experiments.

2.5. Cell Culture and antiproliferative effects

MDA-MB-231 breast adenocarcinoma and HT-29 colon carcinoma were maintained in DMEM high glucose (PAA) supplemented with 50 mg/L gentamycin and 10% (V/V) fetal calf serum (FCS) at 37°C under 5% CO_2 atmosphere and passaged every seven days. Antiproliferative effects were determined essentially as described in a recent publication.[11,20,22] A volume of 100 µl of a 38.000 cells/ml (HT-29) or 40.000 cells/ml (MDA-MB-231) suspension were seeded into 96-well plates and incubated for 48 hours at 37 °C and 5% CO_2. After the incubation period the cells in one plate were fixed by addition of 100 µl of a 10% glutaraldehyde solution and the plate was stored at 4 °C (t_0 plate). Stock solutions of the compounds were freshly prepared in DMF and diluted with cell culture medium to the final concentrations (0.1% v/v DMF). In the remaining plates the medium was replaced by different concentrations of the compound in cell culture medium (6 wells for each concentration). Twelve wells of each plate were treated with a solution of 0.1% DMF in cell culture medium (untreated control). Then the plates were incubated for 72 h (HT-29) or 96 h (MDA-MB-231) at 5% CO_2 and 37 °C. The medium was removed and the cells were treated with 100 µl of a 10% glutaraldehyde solution. Afterwards the cells of all plates were washed with 180 µL PBS and stained with 100 µl of a 0.02% crystal violet solution for 30 minutes. The

crystal violet solution was removed and the plates were washed with water and dried. A volume of 180 µl of ethanol 70% was added to each well and after 3-4 h of gentle shaking the absorbance was measured at 595 nm in a microplate reader (Victor X4, PerkinElmer). The mean absorbance value of the t_0 plate was subtracted from the absorbance values of all other absorbance values. The IC_{50}-values were calculated as the concentrations reducing the cellular proliferation in comparison with the untreated control by 50% and are given as the means and errors of 2 - 3 independent experiments.

2.6. Cellular uptake

For cellular uptake studies cells were grown until at least 70 % confluency in 25 cm^2 cell culture flasks. Stock solutions of the compounds in DMF were freshly prepared and diluted with cell culture medium to the desired concentration of 10 and 50 µM. The cell culture medium of the cell culture flasks was replaced with 3 ml of the cell culture medium containing the gold compound and the flasks were incubated at 37 °C / 5 % CO_2 for 6 h. Subsequent to the incubation period the culture medium was removed and cells were washed with 3 ml PBS. Cells were resuspended in 3 mL PBS by using a cell scratcher and cell pellets were isolated by centrifugation (RT, 3323 g, 5 min). Cellular lysates were prepared by resuspending an isolated cell pellet in 300 µl demineralized water followed by ultrasonication. An aliquot was removed for the purpose of protein quantification by the method of Bradford. The metal content of the samples was determined by high-resolution continuum source atomic absorption spectrometry (HR-CS AAS, see above). To avoid matrix effects matrix-matched calibration was used for gold quantification in the samples. To 20 µl of all injected probes and standards each 2 µl Triton X100 (1 %) were added. Results were calculated from the data of 2-3

independent experiments and are expressed as the cellular molar gold concentration (μM), which was determined as described in a previous report.[33,34]

2.7. Synthesis of Na_3[Au(C≡C-py)(TPPTS)] (1). Solid KOH (5 mg, 0.75 mmol) was added to a solution of NC_5H_4-C≡CH (7 mg, 0.75 mmol) in MeOH (15 ml). After 30 min of stirring at room temperature, solid [AuCl(TPPTS)] (60 mg, 0.75 mmol) was added and the solution was stirred for 2 hours at room temperature. The resulting white solution was concentrated, and diethyl ether (15 ml) was added to precipitate a white solid. The pure compound was obtained by recrystallizing twice the solid dissolved in a H_2O:MeOH mixture, using diethyl ether as the precipitating agent. Yield: 91%. ^{1}H-NMR (400 MHz, D_2O): 8.40 (d, *J* = 12.0 Hz, 2H, H_α-pyr), 7.27 (d, *J* = 12.0 Hz, 2H, H_β-pyr), 7.97-7.95 (m, 6H, H_3, H_6), 7.72-7.63 (m, 6H, H_2, H_4). ^{31}P{^{1}H}-NMR (400 MHz, D_2O): -40.9. IR (KBr, cm^{-1}): 3455 (C-H), 2119 (C≡C), 1588 (C=N). ESI-MS (-) *m/z*: 265.98 $[M - 3H]^{3-}$, 399.47 $[M - 2H]^{2-}$, 410.47 $[M - 3H + Na]^{2-}$, 418.45 $[M - 3H + K]^{2-}$ ($[M]^-$, calc.: 868.50). Anal. Calc. C, 34.69, H, 1.86, N, 1.61, S, 11.09 %; Found C, 34.72, H, 1.88, N, 1.63, S, 11.11 %.

2.8. Synthesis of Na_3[Au(C≡C-$C_{10}H_7O_3$)(TPPTS)] (2). Solid KOH (5 mg, 0.75 mmol) was added to a solution of 7-(prop-2-in-1-yloxy)-1-benzopyran-2-one (15 mg, 0.75 mmol) in MeOH (10 ml). After 30 min of stirring at room temperature, solid [AuCl(TPPTS)] (60 mg, 0.75 mmol) was added and the solution was stirred for 2 hours at room temperature. The resulting yellow solution was concentrated (5 ml) and *n*-hexane (10 ml) was added to precipitate a yellow solid. The pure compound was obtained by recrystallizing twice the solid dissolved in a H_2O:MeOH mixture, using diethyl ether as the precipitating agent. Yield: 83%. ^{1}H-NMR (400 MHz, D_2O): 8.14 (d,

J = 8.0 Hz, 1H, H_3), 8.00-7.81 (m, 6H, $H_{6'}$, $H_{5'}$), 7.73-6.85 (m, 9H, $H_{2'}$, $H_{4'}$ + H_5+ H_8+ H_6), 6.30 (d, *J* = 8.0 Hz, 1H, H_4), 4.44 (s, 2H, H_9). $^{31}P\{^1H\}$-NMR (400 MHz, D_2O): -33.49. IR (KBr, cm^{-1}): 2120 (C≡C), 1730 (C=O). ESI-MS (-) *m/z*: 940.92 $[M - Na]^-$, 458.97 $[(M - 2Na)/2]^{2-}$, 447.97 $[(M - 3Na)/2]^{2-}$, 298.31 $[(M - 3Na)/3]^{3-}$ ($[M]^+$, calc.: 965.60). Anal. Calc. C, 37.36, H, 1.99 %, S, 9.97 %; Found C, 37.38, H, 2.01 %, S, 9.95 %.

2.9. Synthesis of 6,7-bis(prop-2-in-1-yloxy)-1-benzopyran-2-one (PC67)

Solid 6, 7-dihydroxy-1-benzopyran-2-one (300 mg, 1.65 mmol) and K_2CO_3 (570 mg, 4.13 mmol) were mixed in deoxygenated acetone (30 ml). After 5 min of stirring, propargyl bromide (459 μL, 4.13 mmol) was added dropwise and the mixture was refluxed during 5 days. The solution of the reaction was concentrated to dryness, extracted with ethyl acetate–H_2O and recrystallized with ethyl acetate–hexane to give 364 mg of a pale yellow solid in 87% yield. ^{1}H-NMR (400 MHz, 298 K, $CDCl_3$): δ 7.63 (d, 1H, *J* = 9.5 Hz, H3), 7.10 (s, 1H, H8), 7.06 (s, 1H, H5), 6.32 (d, 1H, *J* = 9.5 Hz, H4), 4.83 (d, 2H, *J* = 2.4 Hz, H10), 4.79 (d, 2H, *J* = 2.4 Hz, H9), 2.59 (t, 1H, *J* = 2.4 Hz, H12), 2.55 (t, 1H, *J* = 2.4 Hz, H11). IR (KBr, cm^{-1}): 3266, 3239 (≡C-H), 2216 (C≡C), 1705 (C=O). ESI-MS (+) *m/z*: 255.07 ($[M + H]^+$, calc. 255.06), 277.05 ($[M + Na]^+$, calc. 277.05), 531.10 ($[2M + Na]^+$, calc. 531.12). Anal. Calc. C, 70.86, H, 3.96 %; Found C, 70.89, H, 3.98 %.

2.10. Synthesis of [Au{6,7-bis(prop-2-in-1-yloxy)-1-benzopyran-2-one}$(PTA)_2$] (3)

Solid KOH (27 mg, 0.48 mmol) was added to a mixture of 6,7-bis(prop-2-in-1-yloxy)-1-benzopyran-2-one (60 mg, 0.24 mmol) in methanol (10 ml). After 5 min of stirring a dichloromethane solution (15 ml) of [AuCl(PTA)] (139 mg, 0.34 mmol) was added and

the mixture was maintained at room temperature protected from light with aluminium foil. After 2 hours of stirring, the solution was concentrated to *ca*. 15 ml and hexane (10 ml) was added to precipitate a pale yellow solid. The pure compound was obtained by recrystallizing twice the solid dissolved in a CH_2Cl_2:MeOH mixture, using diethyl ether as the precipitating agent. Yield: 46 % (75 mg). ^{1}H-NMR (400 MHz, 298 K, $CDCl_3$): δ 7.64 (d, 1H, *J* = 9.5 Hz, H3), 7.14 (s, 1H, H8), 7.11 (s, 1H, H5), 6.24 (d, 1H, *J* = 9.5 Hz, H4), 4.88 (s, 2H, H10), 4.85 (s, 2H, H9), 4.55-4.43 (AB q (br), 12H, *J* = 16.0 Hz, N-C*H*$_2$-N), 4.26 (s (br), 12H, N-C*H*$_2$-P). ^{31}P{^{1}H}-NMR (162 MHz, 298 K, $CDCl_3$): δ -51.4 (br). IR (KBr, cm^{-1}): 2127 (C≡C), 1707 (C=O). ESI-MS (+) *m/z*: 961.13 ([M + H]$^+$, calc. 961.14), 983.12 ([M + Na]$^+$, calc. 983.12), 999.09 ([M + K]$^+$, calc. 999.09). Anal. Calc. C, 33.76, H, 3.36, N, 8.75 %; Found C, 33.77, H, 3.39, N, 8.74%.

2.11. Synthesis of [Au{6,7-bis(prop-2-in-1-yloxy)-1-benzopyran-2-one}(DAPTA)$_2$] (4)

Solid KOH (21 mg, 0.37 mmol) was added to a mixture of 6,7-bis(prop-2-in-1-yloxy)-1-benzopyran-2-one (47 mg, 0.19 mmol) in methanol (10 mL). After 5 min of stirring a dichloromethane solution (15 mL) of [AuCl(DAPTA)] (169 mg, 0.36 mmol) was added and the mixture was maintained at room temperature protected from light with aluminium foil and stirred during 24 h. Then, the solution was concentrated to *ca*. 15 mL and hexane (30 mL) was added to precipitate a pale yellow solid. The pure compound was obtained by recrystallizing twice the solid dissolved in a CH_2Cl_2:MeOH mixture, using diethyl ether as the precipitating agent. Yield = 80% (160 mg). ^{1}H-NMR (400 MHz, 298 K, $CDCl_3$): δ 7.62 (d, 1H, *J* = 9.4 Hz, H3), 6.98 (s (br), 2H, H8, H5), 6.27 (d, 1H, *J* = 9.4 Hz, H4), 5.80-5.61 (m (br), 4H, H9, H10), 5.03-4.77 (m (br), 8H, DAPTA), 4.67-4.57 (m (br), 2H, DAPTA) 4.46 (s (br), 2H, DAPTA), 4.26-4.00 (m (br),

6H, DAPTA), 3.84 (s (br), 2H, DAPTA), 2.11 (s (br), 6H, N-CO-CH_3 (DAPTA)), 2.08 (s (br), 6H, N-CO-CH_3 (DAPTA)). $^{31}P\{^1H\}$-NMR (162 MHz, 298 K, $CDCl_3$): δ -24.7 (br). IR (KBr, cm^{-1}): 2125 (C≡C), 1718, 1637 (C=O).ESI-MS (+) *m/z*: 1127.16 ($[M + Na]^+$, calc. 1127.16). Anal. Calc. C, 35.88, H, 3.65, N, 7.61; Found C, 35.91, H, 3.68, N, 7.58 %.

3. Results and Discussion

3.1. Synthesis and Characterization

3.1.1. Synthesis of mononuclear gold(I) derivatives.

In order to analyse the influence of the negatively charged phosphane TPPTS in the spectroscopic and biological properties of Au(I) 4-pyridylethynyl complexes, the complex $Na_3[Au(C{\equiv}C\text{-}py)(TPPTS)]$ was synthesized. The reaction was carried out by deprotonation of the terminal alkynyl proton of the 4-pyridylethynyl ligand with a KOH methanol solution and addition of a stoichiometric amount of [AuCl(TPPTS)] complex (previously synthesized) in the same medium (Scheme 1).

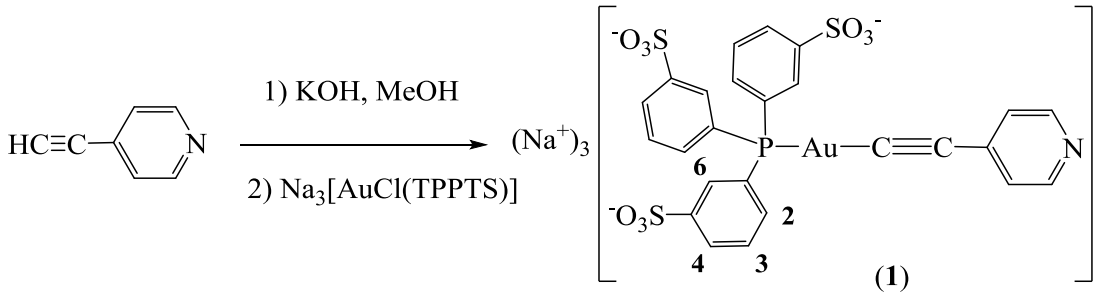

Scheme 1. Synthesis of $Na_3[Au(C{\equiv}C\text{-}py)(TPPTS)]$ (**1**).

The synthesis of this complex was firstly attempted by the reaction of $[Au(C{\equiv}C\text{-}py)]_n$ with the TPPTS phosphine, following the procedure used for the analogous neutral complexes $[Au(C{\equiv}C\text{-}py)(PR_3)]$ (PR_3 = PTA,[25] DAPTA[26]) previously reported by us but the reaction was not accomplished.

The complex $Na_3[Au(C{\equiv}C\text{-}C_{10}H_7O_3)(TPPTS)]$, containing a propargyloxy group instead of pyridylethynyl, was successfully obtained by the same synthethic procedure (Scheme 2) in high yields (80-90%).

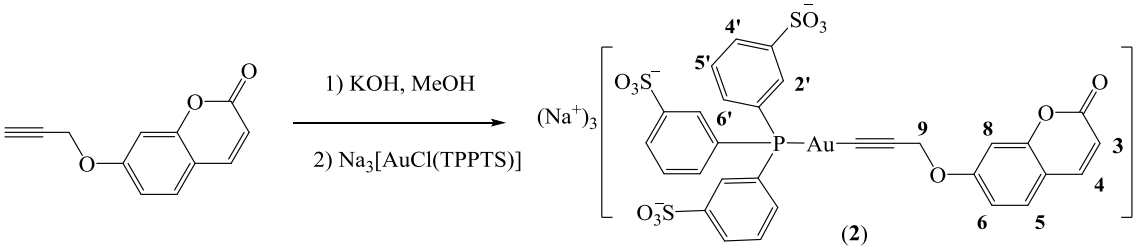

Scheme 2. Synthesis of $Na_3[Au(C{\equiv}C\text{-}C_{10}H_7O_3)(TPPTS)]$ (**2**)

Characterization of the complexes by ^1H and ^{31}P-NMR and IR spectroscopy and ESI(-) mass spectrometry indicates the correct formation of the complexes. The presence of the molecular peak recorded in both cases by ESI-MS(-) indicates the presence of the complexes. IR and ^1H-NMR spectra show the disappearance of the terminal alkynyl proton being a crucial signal of their successful preparation. The presence of the negatively charged phosphane made these complexes highly soluble in polar media (D_2O and DMSO) and almost insoluble in $CDCl_3$, as a difference with the corresponding derivatives with PTA and DAPTA phosphanes.[25,26]

The detailed analysis of the NMR data made us to realise that some kind of aggregates must be present in **1**. In this case, pyridyl protons could only be observed by ^1H-NMR recorded in D_2O at diluted concentrations and these signals were broad and trended to disappear when increasing concentration (Figure 1). ^{31}P-NMR spectrum was also in agreement with the formation of aggregates and displayed two broad peaks with similar chemical environment that become broader when increasing concentration (Figure S3). The formation of these large supramolecular structures was also verified by optical and electronic microscopy (see below).

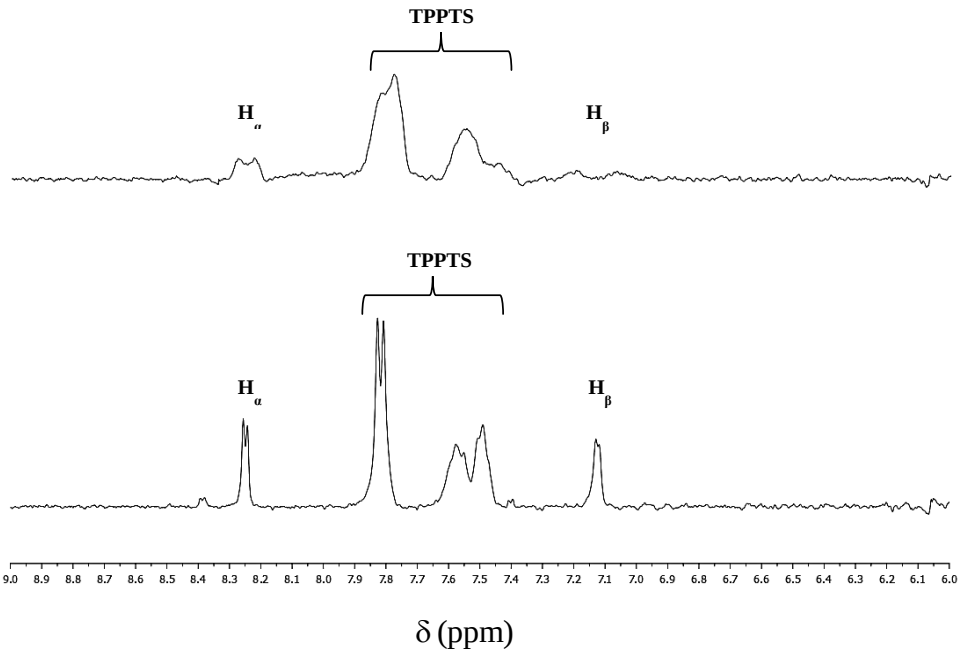

Figure 1. ^{1}H-NMR spectrum of **1** at $1 \cdot 10^{-3}$M (up) and $1 \cdot 10^{-4}$M (bottom) concentrations in D_2O.

3.1.2. Synthesis of dinuclear gold(I) derivatives.

New dinuclear complexes were designed and synthesized in order to analyse how the presence of two metal atoms could affect on their photophysical and aggregation properties and / or could present a cooperative effect on their biological activity. The synthesis of the 6,7-bis(prop-2-in-1-yloxy)-1-benzopyran-2-one (**PC67**) was undertaken following the procedure used for the related compounds containing only one prop-2-in-1-yloxy groups (Scheme S1).[23] 6,7-hydroxycoumarin was made react with propargyl bromide in acetone at 50ºC for 5 days and in the presence of K_2CO_3 to give the corresponding bis-propynyloxycoumarin in pure form after recrystallization in ethyl acetate / hexane (**1**) in very high yield (*ca*. 90%). The reaction of **PC67** with [AuCl(PR_3)] (PR_3 = PTA (**3**), DAPTA (**4**)) in the required stoichiometric conditions led us to obtain the dinuclear complexes **3** and **4** by similar procedure detailed above for mononuclear derivatives (Schemes 3 and S2). Similar reaction was attempted by using

Na_3[AuCl(TPPTS)] derivative but it was not possible to obtain the desired dinuclear complex in pure form.

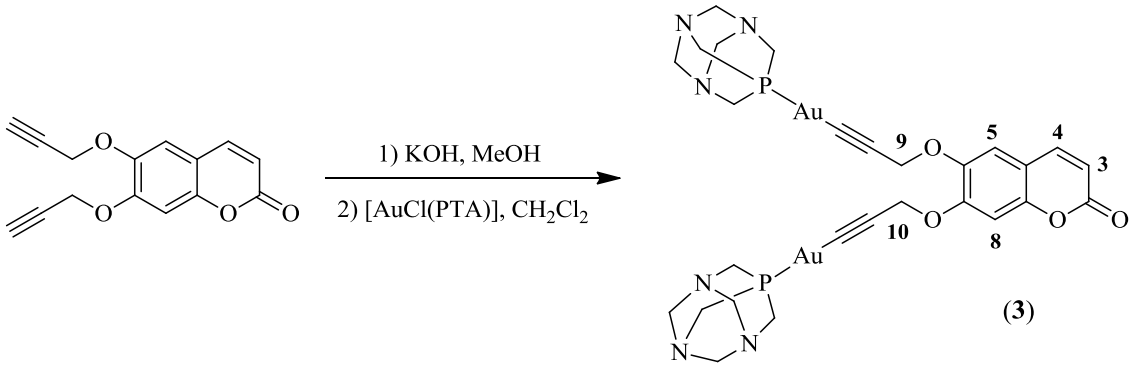

Scheme 3. Synthesis of [Au{6,7-bis(prop-2-in-1-yloxy)-1-benzopyran-2-one}$(PTA)_2$] (**3**).

Characterization of the complexes by ^{1}H and ^{31}P-NMR and IR spectroscopy and ESI(+) mass spectrometry indicates the formation of the complexes. As reported for **1** and **2**, IR and ^{1}H-NMR in $CDCl_3$ show the disappearance of the terminal alkynyl proton being the key point that points out the successful preparation of the complexes. The corresponding protons of the phosphane follow the typical patterns of PTA and DAPTA together with the expected protons of the coumarin unit (Figures S6 and S7). It could be observed that the signals present some broadening due to the slightly unequivalence of both phosphanes and to the possible aggregation effect. This effect is strongly favoured in water, where the compounds display lower solubility, as confirmed by microscopy and photophysical studies (see below). ^{31}P-NMR shows a downfield shift of about -50 ppm for PTA and -20 ppm for DAPTA derivatives respectively, upon coordination of the phosphane to the gold(I) metal atom, as observed for other similar compounds.[18,23,25,26,34]

3.1.3. Dynamic Light Scattering experiments

The presence of aggregates in solution was also evidenced by Dynamic Light Scattering (DLS) experiments in water, in agreement with NMR data. Different concentrations were used in each case depending on the solubility of the complexes in this solvent and are in the range $1 \cdot 10^{-3}$M to $1 \cdot 10^{-5}$M. The results are summarized in Table 1 and Figures S8-S11. As expected, the size of the structures increases with concentration.

Table 1. Size of the aggregates of **1**-**4** in water. [a] The lower solubility of this complex in water precludes the measurement at higher concentration. [b] Two different populations were recorded for this complex.

Compound	Concentration (M)	Size (nm)
1	$1 \cdot 10^{-4}$, $5 \cdot 10^{-4}$	472, 580
2	$1 \cdot 10^{-4}$, $1 \cdot 10^{-3}$	73, 96
3	$2.5 \cdot 10^{-5}$ [a]	275, 903 [b]
4	$5 \cdot 10^{-5}$, $1 \cdot 10^{-4}$	152, 175

As a general trend, it can be observed that complexes **1** and **2**, containing the TPPTS phosphine, are more soluble and the experiments could be undertaken at higher concentrations. The lower interaction between molecules observed by complex **2** is shown by the lower aggregates' size recorded by DLS. Coumarin derivatives containing PTA and DAPTA phosphines (**3** and **4**) aggregate at lower concentrations and, as expected, the lower solubility of the PTA complex in water gives rise to the formation of larger aggregated structures.

This behaviour seems to be maintained in dried samples as observed by optical and electronic microscopy images (see below).

*3.1.4. Characterization by Optical and Electronic Microscopy.*Optical and Scanning Electronic Microscopy have been used to detect the presence of some aggregates in other analogous Au(I) alkynyl derivatives in water and their corresponding sizes and shapes.[25,26,35] For this reason, dried samples of **1**-**4** were deposited adequately to be observed under optical microscopy and SEM (Figure 2). Unfortunately, the small aggregates of **2** preclude their detection by these techniques.

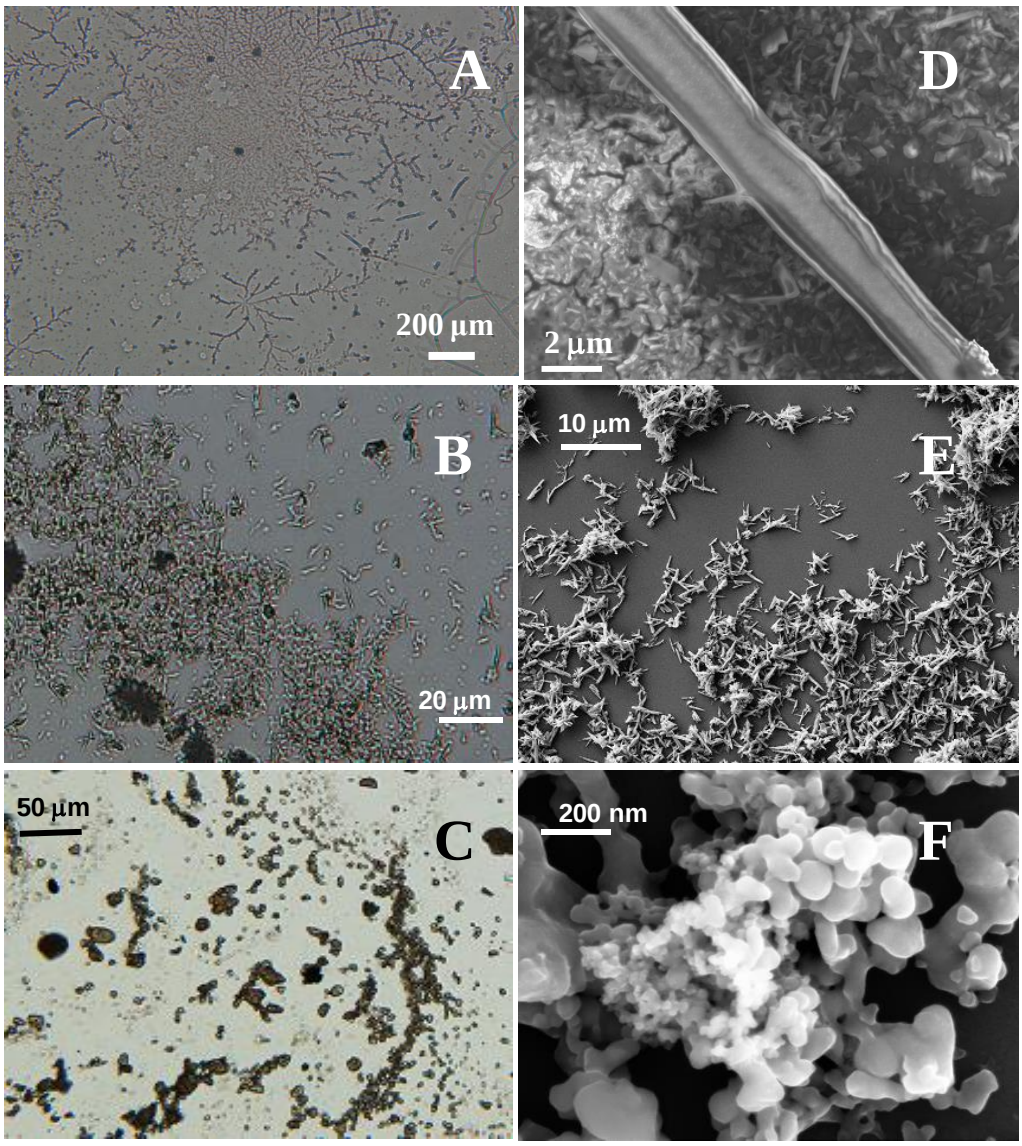

Figure 2. Optical microscopy images of dried samples of **1** (A), **3** (B) and **4** (C) and SEM images of **1** (D), **3** (E) and **4** (F) previously dissolved in water.

Optical and electronic microscopies show the formation of concentric fibrilar structures for **1** that grow from smaller spherical particles. These fibrilar supramolecular assemblies were also observed for the neutral complexes [Au(C≡C-py)(PTA)][25] and [Au(C≡C-py)(DAPTA)],[26] pointing out the key role of the pyridyl moiety on the resulting aggregation motif. On the other hand, complexes **3** and **4** present a different pattern. PTA derivative, **3**, gives rise to the formation of rod-like structures of *ca*. 3 μm length while the higher steric hindrance of the DAPTA phosphine in **4** seem to have a direct role on the formation of smaller and spherical aggregates of *ca*. 100 nm.

Moreover, the presence of two Au-phosphane groups has also a direct influence on the resulting assemblies, since long fibers were very recently observed for the mononuclear [Au{7-(prop-2-ine-1-yloxy)-1-benzopyran-2-one}(DAPTA)] hydrogelator.[27]

3.1.5. Absorption and Emission properties.

The photophysical characterization of Au(I) alkynyl complexes is a denoted research field in gold(I) organometallic chemistry since this property can be used for a wide range of different applications.[24] For this reason, absorption and emission spectra of all complexes were recorded at *ca*. 10^{-5} M concentration and the results are summarized in Table 2. As we were also interested on their potential biological evaluation, these measurements were carried out in water. The absorption, emission and excitation spectra displayed for all complexes resemble those of the relative mononuclear complexes containing the PTA and DAPTA phosphanes.[23] Hence, their photophysical properties are expected to be dependent on the nature of the chromophoric organic part of the molecules.

Table 2. Absorption and emission data of complexes **1-4**. Emission spectra were recorded upon excitation at the lowest energy absorption band. [a]The fluorescence standard reference was quinine sulfate (QY = 0.55, H_2SO_4 0.5 M, 298 K).[1] [b]The fluorescence standard reference was 7-methoxy-4-methylcoumarin (QY = 0.124, MeOH, 298 K).

Compound	Absorption λ_{max} (nm) (10^{-3} ε (M^{-1} cm^{-1}))	Emission (solution, λ_{max} (nm))	QY
1[a]	265 (22.7), 276 (23.5)	410, 430, 442	0.008
2[b]	316 (13.5)	392, 450	0.26
3[b]	298 (8.8), 336 (8.5)	440	0.03
4[b]	300 (10.1), 333 (10.5)	432	0.04

The pyridylethynyl moiety of **1** displays a vibronically structured absorption band assigned to intraligand (IL) π-π* (C≡Cpy) transition.[25,26] This transition displays some broadening which is agreement with that observed in the analogous neutral complexes, where the Au-C≡Cpy moiety is directly involved in the aggregation process. The vibronically structured emission band in **1** (with progressional spacings at *ca.* 2000 cm^{-1}) suggests an intraligand ^{3}[π-π*(alkynyl)] emission origin (Figure 3).

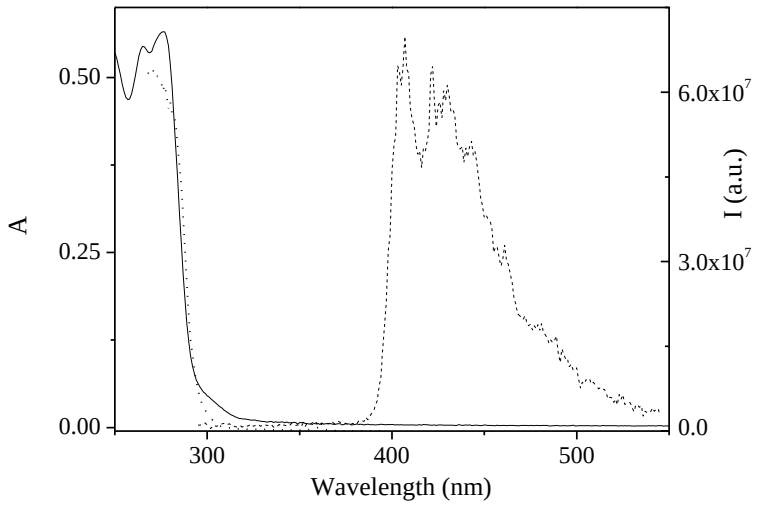

Figure 3. Absorption (solid line); excitation (dotted line, λ_{em} = 470 nm) and emission (dashed line, λ_{exc} = 275 nm) of a $2 \cdot 10^{-5}$M solution of **1** in water.

The coumarin absorption bands of **2-4** are centred at 320-350 nm and present the same profiles. This indicates that the recorded electronic spectra correspond to π–π* transitions of the coumarin group (Figure S12). It is well known that the photophysical properties of the coumarin derivatives can be tuned with small changes in the substituents and their position.[36] Thus, complex **2** (with only one substituent at the 7 position) display a similar shape with a blue shifted band in comparison with that recorded for **3** and **4** (with two substituents at 6 and 7 position). Similar extinction coefficients were recorded in comparison with the mononuclear derivatives previously reported,[23] in agreement with the presence of only one coumarin chromophoric unit.

Emission spectra recorded upon excitation of all the samples at the lowest energy band display two different profiles (Figure 4). Two broad emission bands centered at 392 and 450 nm were recorded for the mononuclear complex, **2**, while a single broad emission band centered at *ca*. 440 nm was observed for the dinuclear complexes **3** and **4**.

Excitation spectra collected at the emission maxima reproduce absorption of the coumarin units (Figure 4), which is indicative of the origin of these emission bands. The large Stokes' shift of all the lowest energy emission bands and the comparison with other coumarin derivatives,[23] make us to assign the emission as phosphorescence of the coumarin which could be favoured by the presence of the gold metal atoms (heavy atom effect) that induces population of the triplet emissive state. Moreover, the highest energy emission band recorded for **2** (392 nm) corresponds to fluorescence of the coumarin unit. Thus, this is a nice example about how the heavy atom effect makes a direct influence on the intersystem crossing and induces phosphorescence, being more favoured when the molecule contains two gold metal atoms.

On the other hand, the emission spectra of **3** and **4** are broader than the recorded for **2**, being in agreement with the presence of more aggregated structures in the sample that are the responsible of their photophysical properties.

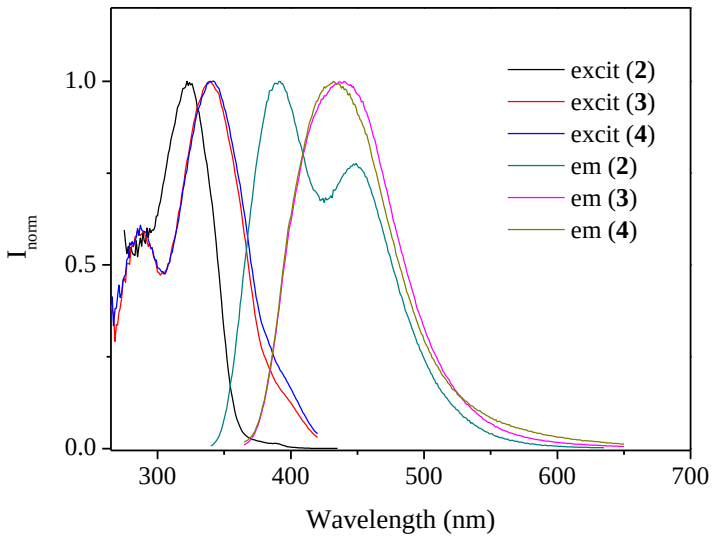

Figure 4. Normalized excitation (collected at emission maxima) and emission spectra (excitation at the absorption maxima) of $2 \cdot 10^{-5}$ M solutions of **2-4** in water.

Total luminescence quantum yields were measured related to quinine sulphate or 7-methoxy-4-methylcoumarin and demonstrate that coumarin derivatives present stronger luminescent than complex **1**, containing pyridyl unit. Especially relevant is the high value measured for **2** that makes it suitable candidate to be used as fluorescent marker in cells (see below).

3.2. Biological studies

The biological evaluation was focused on determining the effects against tumor cell growth in HT-29 colon carcinoma and MDA-MB-231 breast cancer (Table 3), the inhibitory potency against the enzyme thioredoxin reductase and the cellular uptake into MDA-MB-231 cancer cells.

Table 3. IC_{50} values for cytotoxicity in HT-29 and MDA-MB-231 cells; n.d., not determined. Mean values ± errors of 2 - 3 independent experiments.

Complex	MDA-MB-231	HT-29
1	> 100 µM	> 100 µM
2	> 50 µM	> 100 µM
3	51.78 ±0.69 µM	> 75 µM
4	> 100 µM	> 100 µM

With the exception of a moderate cytotoxic effect of **3** against MDA-MB-231 cells, the complexes did not trigger significant cell growth inhibitory effects. This may be related to the above described aggregation effects that had hampered the biological assays concerning solubility in aqueous environment at higher dosages.

In order to clarify the bioavailability of the complexes under cell culture conditions we determined the cellular gold uptake by atomic absorption spectroscopy (Figure 5).[34] The cellular uptake behaviour of a compound is strongly influenced by its lipophilicity. A rather lipophilic neutral complex can easily penetrate the cell membranes by passive diffusion. Complexes **1** and **2** are charged species but also lipophilic. The highest intracellular gold levels could be observed for **1** indicating that the pyridylethynyl unit is more beneficial for cell membrane penetration than the propargyloxycoumarin moiety which is present in the complexes **2**-**4**. However, in comparison with previous results the levels obtained with **1** are comparably low despite the rather high exposure concentrations of 10 and 50 µM.[20,33,37] Cellular gold levels for **2**-**4** were barely detectable. Taken together, this indicates that low bioavailability is the main reason for the missing (low) cytotoxicity of the complexes under study.

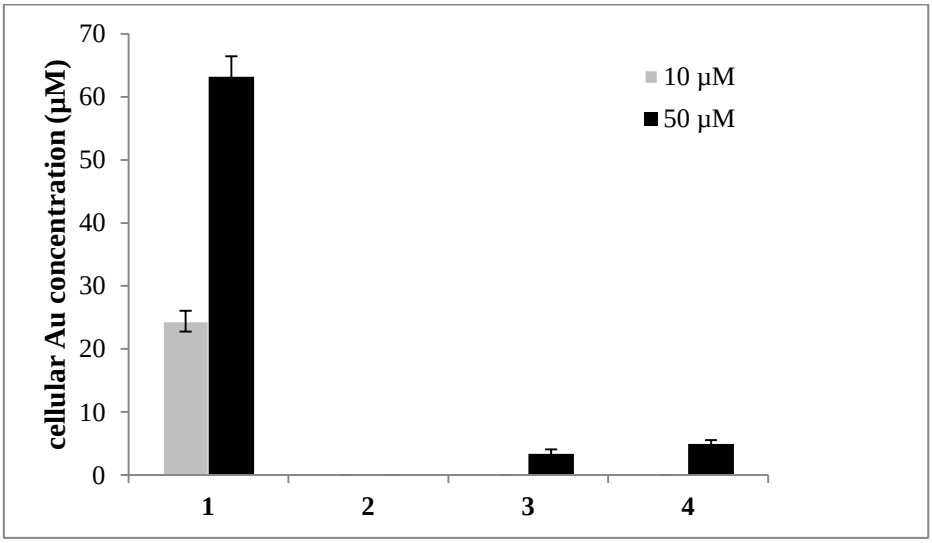

Figure 5. Cellular gold accumulation in MDA-MB-231 cells after 6 h exposure to 10 and 50 µM of the complexes **1** – **4**. Mean values ± errors of 2 – 3 independent experiments. Cellular uptake of **2** was not detectable.

Related to our previous studies, which had shown strong TrxR inhibition for several gold alkynyl complexes, we studied the effects of **1**-**4** on TrxR activity. For this purpose

we screened all complexes in a pilot experiment and determined an exact IC_{50} values for the most active complex **2**. The obtained value of 0.055±0.017 μM for TrxR inhibition by **2** agrees well with the previously reported strong inhibitory potency of gold(I) alkynyl complexes.[20,33]

The relevant role of the presence of two metal atoms of **3** and **4** should be highlighted in comparison with previous studies carried out with mononuclear PTA and DAPTA phosphines containing the same chromophoric unit.[23] The very low biological activity of the complexes herein reported demonstrates the direct effect of the presence of two Au-phosphine units in the chemical structure of **3** and **4** in the studied processes with a significant decrease on the IC_{50} values and TrxR inhibition.

4. Conclusions

The synthesis of new organometallic gold(I) derivatives containing an alkynyl unit with a pyridyl or propargyloxycoumarin chromophore and water soluble phosphanes at second coordinative position of the metal atom has given rise to the formation of water soluble complexes. Characterization by NMR and microscopy show the formation of well organized aggregates in water.

The analysis of their photophysical properties shows that the species display emission from the chromophoric unit in all cases. Moreover, the presence of the gold heavy atom induces the population of the triplet state and hence, phosphorescence emission. This intersystem crossing is more favoured for the dinuclear complexes (two heavy atoms in the molecule).

The biological screening showed low / missing cytotoxic effects. This is most likely related to the low bioavailability as evidenced by measuring the cellular gold levels using atomic absorption spectroscopy. On the other hand, comparison with previous data obtained for analogous mononuclear complexes containing PTA or DAPTA phosphines[23] indicated that structure activity relationships regarding the potential cytotoxic activity could be related to the energy for Au-P bond dissociation. The higher measured IC_{50} values could be directly related to the more difficult process to cleavage the Au-P bond and the involvement of this step in the biological activity. In the case of complexes **1** and **2**, the presence of the anionic phosphine TPPTS increases the electron density of the Au-P. In the case of **3** and **4**, the presence of two phosphine-Au-alkynyl arms coordinated to the coumarin chromophore (instead of one in Au{7-(prop-2-in-1-yloxy)-1-benzopyran-2-one}-(phosph)] (phosph = PTA, DAPTA)[23]) may be the reason for the increasing of the IC_{50} value. This fact could be an important factor to consider in the design of new phosphine-gold(I)-alkynyl complexes.

For complex **2** strong inhibition of the target enzyme TrxR was confirmed. However, due to its very low (missing) cellular uptake the strong TrxR inhibition by **2** did not translate into cytotoxic effects in the proliferation assays. Future studies should therefore focus on improving the bioavailability of the complexes while maintaining their strong TrxR inhibition.

The luminescent properties of our complexes together with their lack of cytotoxicity make them important candidates to be used as fluorescent markers, mainly complex **2**.

5. Supporting Information

Synthesis of 6,7-bis(prop-2-in-1-yloxy)-1-benzopyran-2-one (**PC67**) (Scheme S1); Synthesis of [Au{6,7-bis(prop-2-in-1-yloxy)-1-benzopyran-2-one}$(DAPTA)_2$] (**4**) (Scheme S2); HR-ESI(-) mass spectrum of Na_3[Au(C≡C-C_5H_4N)(TPPTS)] (**1**) (Figure S1); HR-ESI(-) mass spectrum for the compound Na_3[Au(C≡C-$C_{10}H_7O_3$)(TPPTS)] (**2**) (Figure S2); ^{1}H-NMR spectrum of **1** at $1\cdot10^{-3}$M (up) and $1\cdot10^{-4}$M (bottom) concentrations in D_2O (Figure S3); HR-ESI(-) mass spectrum for the compound [Au{6,7-bis(prop-2-in-1-yloxy)-1-benzopyran-2-one}$(PTA)_2$] (**3**) (Figure S4); HR-ESI(-) mass spectrum for the compound [Au{6,7-bis(prop-2-in-1-yloxy)-1-benzopyran-2-one}$(DAPTA)_2$] (**4**) (Figure S5); ^{1}H-NMR spectrum of [Au{6,7-bis(prop-2-in-1-yloxy)-1-benzopyran-2-one}$(PTA)_2$] (**3**) in $CDCl_3$ (Figure S6); ^{1}H-NMR spectrum of [Au{6,7-bis(prop-2-in-1-yloxy)-1-benzopyran-2-one}$(DAPTA)_2$] (**4**) in $CDCl_3$ (Figure S7); DLS measurements of **1** in water at $1\cdot10^{-4}$M and $5\cdot10^{-4}$M concentrations (Figure S8); DLS measurements of **2** in water at $1\cdot10^{-4}$M and $1\cdot10^{-3}$M concentrations (Figure S9); DLS measurements of **3** in water at $2.5\cdot10^{-5}$M concentration (Figure S10); DLS measurements of **4** in water at $5\cdot10^{-5}$M and $1\cdot10^{-4}$M concentrations (Figure S11); Normalized absorption spectra of **2**-**4** in water (Figure S12).

6. Acknowledgements

The support and sponsorship provided by COST Action CM1105 is acknowledged. Authors are also grateful to the Ministerio de Ciencia e Innovación of Spain (Project ENE2012-36368) and the Deutsche Forschungsgemeinschaft (DFG). J.Ll. is Serra Húnter Fellow and is grateful to ICREA Academia program. This research was supported by a Marie Curie Intra European Fellowship within the 7th European Community Framework Programme (R.G.).

7. References

[1] T. Zou, Ching T. Lum, C.-N. Lok, J.-J. Zhang, C.-M. Che, Chem. Soc. Rev. 44 (2015) 8786.

[2] I. Ott, Coord. Chem. Rev. 253 (2009) 1670.

[3] A. Gutiérrez, I. Marzo, C. Cativiela, A. Laguna, M. C. Gimeno, Chem. Eur. J. 21 (2015) 11088

[4] T. V. Serebryanskaya, A.S. Lyakhov, L.S. Ivashkevich, J. Schur, C. Frias, A. Prokop, I. Ott, Dalton Trans. 44 (2015) 1161.

[5] L. Messori, F. Scaletti, L. Massai, M.A. Cinellu, C. Gabbiani, A. Vergara, A. Merlino, Chem. Commun. 49 *(*2013) 10100.

[6] M. J. McKeage, L. Maharaj and S. J. Berners-Price, Coord. Chem. Rev. 232 (2002), 127.

[7] A. Bindoli, M. P. Rigobello, G. Scutarib, C. Gabbiani, A. Casini and L. Messori, Coord. Chem. Rev. 253 (2009) 1692

[8] V. Gandin, A. P. Fernandes, M. P. Rigobello, B. Dani, F. Sorrentino, F. Tisato, M. Bjornstedt, A. Bindoli, A. Sturaro, R. Rella and C. Marzano, Biochem. Pharmacol. 79 (2012) 90.

[9] C. Gabbiani and L. Messori, Anticancer Agents Med. Chem. 11 (2011) 929.

[10] S.Medici, M. Peana, V.M. Nurchi, J.I. Lachowicz,G. Crisponi, M.A. Zoroddu, Coord. Chem. Rev. 284 (2015) 329.

[11] R. Rubbiani, E. Schuh, A. Meyer, J. Lemke, J. Wimberg, N. Metzler-Nolte, F. Meyer, F. Mohr, I. Ott, Med. Chem. Comm. 4 (2013) 942.

[12] B. Bertrand, L. Stefan, M. Pirrotta, D. Monchaud, E. Bodio, P. Richard, P. Le Gendre, E. Warmerdam, M. H. de Jager, G. M. M. Groothuis,M. Picquet, A. Casini, Inorg. Chem. 53 (2014) 2296.

[13] A. Citta, E. Schuh, F. Mohr, A. Folda, M. L. Massimino, A. Bindoli, A. Casini, M. P. Rigobello Metallomics 5 (2013) 1006.

[14] J. Arcau, V. Andermark, M. Rodrigues, I. Giannicchi, Ll. Pérez-Garcia, I. Ott, L. Rodríguez Eur. J. Inorg. Chem. (2014) 6117.

[15] J.C. Lima, L. Rodríguez Anticancer Ag. Med. Chem. 11 (2011) 921.

[16] U.E. Horvath, L. Dobrzanska, C.E. Strasser, W. Bouwer Nee Potgieter, G. Joone,C.E. van Rensburg, S. Cronje, H.G. Raubenheimer, J. Inorg. Biochem. 111 (2012) 80.

[17] B. Bertrand, A. Casini, Dalton Trans. 43 (2014) 4209.

[18] E. Vergara, E. Cerrada, A. Casini, O. Zava, M. Laguna and P. J. Dyson, Organometallics 29 (2010) 2596.

[19] E. Schuh, S. M. Valiahdi, M. A. Jakupec, B. K. Keppler, P. Chiba and F. Mohr, Dalton Trans. (2009) 10841.

[20] A. Meyer, C. P. Bagowski, M. Kokoschka, M. Stefanopoulou, H. Alborzinia, S. Can, D. H. Vlecken, W. S. Sheldrick, S. Wölfl and I. Ott Angew. Chem., Int. Ed. 51 (2012) 8895.

[21] C.-H. Chui, R.-M. Wong, R. Gambari, G. Y.-M. Cheng, M. C.-W. Yuen, K.-W. Chan, S.-W. Tong, F.-Y. Lau, P. B.- S. Lai, K.-H. Lam, C.-L. Ho, C.-W. Kan, K. S.-Y. Leung and W.-Y. Wong, Bioorg. Med. Chem. 17 (2009) 7872.

[22] A. Meyer, A. Gutiérrez, I. Ott and L. Rodríguez, Inorg. Chim. Acta 398 (2013) 72.

[23] J. Arcau, V. Andermark, E. Aguiló, A. Gandioso, A. Moro, M. Cetina, J.C. Lima, K. Rissanen, I. Ott, L. Rodríguez, Dalton Trans. 43 (2014) 4426.

[24] J.C. Lima, L. Rodriguez, Chem. Soc. Rev. 40 (2011) 5442.

[25] R. Gavara, J. Llorca, J. C. Lima and L. Rodríguez, Chem. Commun. 49 (2013) 72.

[26] E. Aguiló, R. Gavara, J. C. Lima, J. Llorca and L. Rodríguez, J. Mater. Chem. C, 1 (2013) 5538.

[27] A.J. Moro, B. Rome, E. Aguiló, J. Arcau, R. Puttreddy, K. Rissanen, J.C. Lima, L. Rodríguez, Org. Biomol. Chem. 13 (2015) 2026.

[28] L. Dellaciana and A. Haim, J. Heterocycl. Chem., 21 **(**1984) 607.

[29] S. Sanz, L. A. Jones, F. Mohr and M. Laguna, Organometallics, 26 (2007) 952.

[30] Z. Assefa, B.G. McBurnett, R.J. Staples, J.P. Fackler, B. Assmann, K. Angermaier, H. Schmidbaur, Inorg. Chem. 34 (1995) 75.

[31] M. Ferrer, M. Mounir, L. Rodríguez, O. Rossell, S. Coco, P. Gómez-Sal, A. Martin, J. Organomet. Chem. 690 (2005) 2200.

[32] R. Rubbiani, S. Can, I. Kitanovic, H. Alborzinia, M. Stefanopoulou, M. Kokoschka, S. Mönchgesang, W.S. Sheldrick, S. Wölfl and I. Ott, J. Med. Chem. 54 (2011) 8646.

[33] I. Ott, H. Scheffler, R. Gust. Chem. Med. Chem. 2 (2007) 702.

[34] I. Ott, C. Biot, C. Hartinger, AAS, XRF and MS Methods in Chemical Biology of Metal Complexes. In: Inorganic Chemical Biology: Principles, Techniques and Applications, John Wiley & Sons, Ltd, UK, (2014), ISBN: 978-1-11851-002-5.

[35] E. García-Moreno, S. Gascón, M. J. Rodriguez-Yoldi, E. Cerrada and M. Laguna, Organometallics 32 (2013) 3710.

[36] E. Y.-H. Hong, H.-L. Wong and V. W.-W. Yam, Chem. Eur. J. 21 (2015) 5732.

[37] J. S. Seixas de Melo, R. S. Becker and A. L. Maçanita, J. Phys. Chem., 98 (1994) 6054.

[38] H. Scheffler, Y. You I. Ott, Polyhedron 29 (2010) 66.